Patient-derived melanoma organoid models facilitate the assessment of immunotherapies

Lingling Ou,[a,b] Shujing Liu,[a] Huaishan Wang,[a] Yeye Guo,[a] Lei Guan,[c] Longbin Shen,[d] Ruhui Luo,[b] David E. Elder,[a] Alexander C. Huang,[e] Giorgos Karakousis,[f] John Miura,[f] Tara Mitchell,[e] Lynn Schuchter,[e] Ravi Amaravadi,[e] Ahron Flowers,[e] Haiwei Mou,[g] Fan Yi,[h] Wei Guo,[c] Jina Ko,[a] Qing Chen,[g] Bin Tian,[g] Meenhard Herlyn,[g] and Xiaowei Xu[a,*]

[a]Department of Pathology and Laboratory Medicine, University of Pennsylvania, Philadelphia, PA, 19104, USA
[b]Stomatological Hospital, School of Stomatology, Southern Medical University, Guangzhou, 510280, China
[c]Department of Biology, University of Pennsylvania, Philadelphia, PA, 19104, USA
[d]The First Affiliated Hospital of Jinan University, Guangzhou, 510632, China
[e]Department of Medicine, University of Pennsylvania, Philadelphia, PA, 19104, USA
[f]Department of Surgery, University of Pennsylvania, Philadelphia, PA, 19104, USA
[g]The Wistar Institute, Philadelphia, PA, 19104, USA
[h]Department of Radiation Oncology, University of Pennsylvania, Philadelphia, PA, 19104, USA

eBioMedicine
2023;92: 104614
Published Online 23 May 2023
https://doi.org/10.1016/j.ebiom.2023.104614

Summary

Background Only a minority of melanoma patients experience durable responses to immunotherapies due to inter- and intra-tumoral heterogeneity in melanoma. As a result, there is a pressing need for suitable preclinical models to investigate resistance mechanisms and enhance treatment efficacy.

Methods Here, we report two different methods for generating melanoma patient-derived organoids (MPDOs), one is embedded in collagen gel, and the other is inlaid in Matrigel. MPDOs in Matrigel are used for assessing the therapeutic effects of anti-PD-1 antibodies (αPD-1), autochthonous tumor infiltrating lymphocytes (TILs), and small molecule compounds. MPDOs in collagen gel are used for evaluating the chemotaxis and migratory capacity of TILs.

Finding The MPDOs in collagen gel and Matrigel have similar morphology and immune cell composition to their parental melanoma tissues. MPDOs show inter- and intra-tumoral heterogeneity and contain diverse immune cells such as $CD4^+$, $CD8^+$ T, Treg, $CD14^+$ monocytic, $CD15^+$, and $CD11b^+$ myeloid cells. The tumor microenvironment (TME) in MPDOs is highly immunosuppressive, and the lymphoid and myeloid lineages express similar levels of PD-1, PD-L1, and CTLA-4 as their parental melanoma tissues. Anti-PD-1 antibodies (αPD-1) reinvigorate $CD8^+$ T cells and induce melanoma cell death in the MPDOs. TILs expanded by IL-2 and αPD-1 show significantly lower expression of TIM-3, better migratory capacity and infiltration of autochthonous MPDOs, and more effective killing of melanoma cells than TILs expanded by IL-2 alone or IL-2 with αCD3. A small molecule screen discovers that Navitoclax increases the cytotoxicity of TIL therapy.

Interpretation MPDOs may be used to test immune checkpoint inhibitors and cellular and targeted therapies.

Funding This work was supported by the NIH grants CA114046, CA261608, CA258113, and the Tara Miller Melanoma Foundation.

Keywords: Melanoma patient-derived organoids (MPDOs); Tumor microenvironment (TME); Tumor infiltrating lymphocytes (TILs); Anti-PD-1 antibodies; Small molecule inhibitor

Introduction

Melanoma is one of the most aggressive cancers with significant mortality.[1] Several treatments are currently available for melanoma, including checkpoint blockade immunotherapy, targeted therapy, and TIL therapy, which have proven effective.[2,3] However, a majority of patients fail to respond or develop resistance quickly. The root cause of this resistance lies in the inter- and

*Corresponding author. Department of Pathology and Laboratory Medicine, University of Pennsylvania, 6th Founders Building, 3400 Spruce Street, Philadelphia, PA, 19104.
E-mail address: xug@pennmedicine.upenn.edu (X. Xu).

Research in context

Evidence before this study

Melanoma is a highly aggressive cancer with significant mortality rates. Unfortunately, the majority of patients do not respond to immunotherapy due to the inter- and intra-tumoral heterogeneity in melanoma. Appropriate preclinical models are urgently needed to test treatment efficacy and understand resistance mechanisms. However, traditional cell lines and animal models have limitations in studying the native tumor immune microenvironment. As a result, there is an urgent need for new, personalized models to test immunotherapy for melanoma.

Added value of this study

Our findings indicate that MPDOs in collagen gel and Matrigel display inter- and intra-tumoral heterogeneity, and comprise diverse immune cells, contributing to a highly immunosuppressive tumor microenvironment. MPDOs present a convenient method for testing αPD-1 blocking, assessing autochthonous TILs migration and killing efficiency, and screening small molecules.

Implications of all the available evidence

Our study indicates that MPDOs have the potential to serve as a platform for investigating treatment resistance mechanisms and testing different therapeutic modalities.

intra-tumoral heterogeneity, which affects the treatment response.[4]

Animal models, including patient-derived xenografts (PDX), have limitations due to their inability to replicate the native tumor immune microenvironment, prolonged tumor generation duration (2–11 months), and host mouse immune cell infiltration into the tumor. The success rate of translating cancer therapies from animal models to human patients is less than 10%.[5] Three-dimensional (3D) organoids have emerged as a promising alternative to PDX models, as they avoid some limitations.[6,7] Organoid culture also shows several advantages over monolayer, tumor cell line spheroids,[8,9] and circulating tumor cells (CTCs).[10] Recently, organoid culture systems have been developed from various patient tumor types,[11–14] providing a platform that recapitulates the phenotypic and molecular heterogeneity of the tumor. Patient-derived organoids (PDOs) can be grown from dissociated tumor tissues in Matrigel,[15] collagen gel,[14] microfluidic culture device,[16] or air-liquid interface.[17,18]

Melanoma has a unique tumor microenvironment (TME), which frequently contains an abundance of tumor-infiltrating immune cells and stromal cells[19] that influence both melanoma progression and treatment response.[20,21] Melanoma patient-derived organoids (MPDOs) have recently been established using fine needle aspiration material.[22] Despite their potential, few studies have compared different PDO culture methods and thoroughly characterized the immune cells within the PDOs.

This study reports two different methods for culturing MPDOs that replicate the melanoma TME. Dissociated melanoma tissues were inlaid in Matrigel or embedded in collagen gel. The resulting MPDOs demonstrated intertumoral heterogeneity and contained diverse immune cells. We tested the efficacy of αPD-1 in activating $CD8^+$ T cells and inducing tumor cell death in MPDOs. We discovered that TIL expanded by IL-2 and αPD-1 infiltrated MPDOs better and killed melanoma cells more effectively than other methods. We found navitoclax increased the treatment efficacy of TILs through a small molecule screening assay. MPDOs offer a platform to study the mechanisms underlying heterogeneous clinical results after checkpoint blockade[23] and test different immunotherapies.

Methods

Fresh human melanoma and MPDO culture

Human melanoma tissues were obtained from patients receiving treatment using the tissue collection protocol (UPCC08607) that is approved by the Institutional Review Board of University of Pennsylvania. All patients have signed informed consents. Samples were obtained from adult male or female patients (ages arranged from 26 to 86), and no differences in organoid formation capacity in male and female samples were observed. Out of 30 patient samples collected, 22 were successful in growing organoids, and patient information is listed in Table S1. PBMCs were isolated from the peripheral blood of healthy donors provided by the Human Immunology Core at the University of Pennsylvania with informed consent and ethical approval (Protocol number 707906).

All surgical samples were confirmed to be melanoma before processing. Melanoma tissues were washed with PBS (containing 2% penicillin/streptomycin (P/S)) and minced finely on ice. Fragments were digested in 5 ml RPMI 1640 medium containing collagenase IV (200 U/ml, Sigma–Aldrich) and DNase I (50 U/ml, Sigma–Aldrich) for 30 min at 37 °C, diluted by 20 ml complete RPMI 1640 medium and filtered over 100 μm strainers.

Two culture methods were used to cultivate dissociated melanoma tissues. One method was the air-liquid culture system as described.[24] 1 ml collagen gel (Trevigen) was lay on inner transwell inserts to solidify, and then 1×10^6 cells derived from digested tissues mixed in 1 ml collagen gel were layered on top of pre-solidified collagen gel. The transwell inserts containing

cells and collagen were placed into 6-well plates with the fluid level of the culture medium equal to the top of the collagen gel. The culture medium contained 40% ADMEM/F12 medium, 50% Wnt3a, RSPO1, Noggin-conditioned media (L-WRN, ATCC), and 10% inactivated fetal calf serum, supplemented with 1 mM HEPES (Invitrogen), 1 × Glutamax (Invitrogen), 10 mM Nicotinamide (Sigma), 1 mM N-Acetylcysteine (Sigma), 1 × B27 without vitamin A (Invitrogen), 0.5 μM A83-01 (Tocris), 1 × Pen-Strep Glutamine (Invitrogen), 10 nM Gastrin (Sigma), 10 μM SB-202190 (Sigma), 50 ng/ml EGF (Peprotech) and 50 ng/ml FGF-1 (R&D Systems). The passage of organoids was performed every 5–7 days using collagenase IV (200 units/ml) for digestion at 37 °C for 20 min, and split into 1:3 in new wells. In some experiments, culture medium was supplemented with recombinant human IL-2 (Peprotech, 600 IU/ml) or αPD-1 (pembrolizumab, 75 μg/ml) as indicated.[24]

Another culture method was single-cell suspension seeded on a Matrigel (Corning) bed as described.[25] The Matrigel was mixed with complete DMEM/F12 medium at a 1:2 ratio and put in the wells in a 6-well plate, allowing to solidify. The tumor cell mixture (1×10^6 cells) was seeded on the Matrigel surface, then cultured up to 7–14 days for subsequent analyses, the medium was changed every three days. Organoids were passaged every 5–7 days by washing with cold Advanced DMEM/F12 medium and digested by TrypLE Express (Gibco). The culture medium was supplemented with 600 IU/ml IL-2 or 75 μg/ml αPD-1 in some cases. Successful establishment of melanoma organoid cultures was defined by the spheroid-like 3D structure, multiple cellular components in the organoids, and the ability of organoids to grow bigger and passage for at least 1–2 times. For cryopreservation, MPDOs were resuspended in a freezing medium supplemented with 90% inactivated fetal calf serum and 10% DMSO. For recovery, cryovials with MPDOs were quickly thawed in a 37 °C water bath.

Generation of organoids from melanoma tissue fragments

Fresh melanoma tumor tissues (17 samples) were cut into small pieces of 0.5–1 mm and placed in 6-well culture plates supplemented with complete ADMEM/F12 medium containing 10% inactivated fetal calf serum, 50% Wnt3a, RSPO1, Noggin-conditioned media with 1 mM HEPES, 1 × Glutamax, 10 mM Nicotinamide, 1 mM N-Acetylcysteine, 1 × B27 without vitamin A, 0.5 μM A83-01, 1 × Pen-Strep Glutamine, 10 nM Gastrin, 10 μM SB-202190, 50 ng/ml EGF and 50 ng/ml FGF-1. About 75% of the medium was changed every three days. Cells were migrated from the tumor pieces during the culture period within 1–2 weeks. The criteria for successful organoid generation were the tumor pieces survived for two weeks, a spherical morphology, and continuously grew in culture.[26]

TIL expansion from tumor fragments

TIL used for this study was generated as previously described.[27] Briefly, fresh melanoma tumor was dissected into 1–2 mm^3 fragments, and placed in wells of a 24-well plate, maintained in RPMI medium supplemented with 15% inactivated fetal calf serum, 2 mM L-glutamine, 25 mM HEPES, 1 × Pen-Strep Glutamine and IL-2 (600 IU/ml). The expanded TILs were activated by supplementing with 2 μg/ml αCD3 antibodies or αPD-1 (pembrolizumab, 75 μg/ml) for 24 h. TILs were grown for 7–14 days and prepared for subsequent analysis.

For analyzing TIL migration, MPDOs (3×10^5 cells) were embedded in the collagen 3D matrices using an air-liquid culture system placed in a 24-well plate, and 1×10^6 viable TILs (prelabeled with CFSE) were added on the top of collagen gel. TILs migrated to organoids in the bottom and the movement of TILs was imaged by Zeiss LSM 710 Confocal microscopy (Carl Zeiss, Germany) after 1 h of addition of TILs at 37 °C, 5% CO_2. Time-lapse imaging was captured every hour for 24 h. The velocity of TILs was quantified.

For analyzing TIL infiltration and direct killing ability, MPDOs (2×10^5 cells) were seeded and grown semi-immersion in Matrigel, and 1×10^6 viable TILs (prelabeled with CFSE or not) were added and co-cultured with MPDOs. Confocal microscopy was used to observe TIL-tumor cell contact.

Histological analysis and immunofluorescence study

For immunofluorescence and H&E analysis, MPDOs in collagen gel were embedded in OCT and sectioned into 25 μm, followed by fixation with 4% paraformaldehyde for 30 min. MPDOs in Matrigel were analyzed using whole mount staining without sectioning for subsequent staining. The following primary antibodies were used: anti-α-SMA (Abcam, ab5694, 1:200), anti-vimentin (Cell Signaling Technology, 5741S, 1:200), anti-ICAM-1 (Proteintech, 10020-1-AP, 1:200), anti-HMB-45 (Abcam, ab733, 1:200), anti-CD45 (CST, 13917S, 1:200), anti-CD3e (Proteintech, 60181-1-Ig, 1:200), anti-CD8a (Abcam, ab4055, 1:200), anti-CD14 (Proteintech, 17000-1-AP, 1:200), anti-CD11b (Novus Biologicals, NB110-89474, 1:200) and anti-PD-L1 (CST, 13684S, 1:200). The primary antibodies were incubated overnight at 4 °C and followed by secondary antibodies incubated with Alexa Fluor 488 (1:500 dilutions; CST), Alexa Fluor 555 (1:500 dilutions; CST) and Alexa Fluor 647 (1:500 dilutions; Invitrogen)-conjugated secondary antibodies for 1 h at room temperature. Nuclei were stained with DAPI (1:1000 dilutions; Invitrogen) for 15 min, and images were captured using a Zeiss LSM 710 Confocal microscopy.

Flow cytometric immune profiling of MPDOs and melanoma tumor samples

To evaluate the immune cells in MPDOs or fresh tumor samples, organoids or tumor samples were dissociated

into single cells. The single-cell suspension (1×10^6 cells) was used for staining and FACS analysis. Antibodies were used as follow: anti-CD45 (HI30), anti-CD3 (OKT3), anti-CD4 (OKT4), anti-CD8 (SK1), anti-CD14 (63D3), anti-CD11b (ICRF44), anti-CD68 (Y1/82A), anti-CD15 (W6D3), anti-HLA-DR (G46-6), anti-CD33 (P67.6), anti-PD-1 (EH12.1), anti-CTLA4 (BNI3), anti-PD-L1 (10F.9G2), anti-CD25 (BC96), anti-Foxp3 (206D), anti-IFN-γ (B27), anti-Ki67 (Ki67), and IgG1 isotype control from Biolegend. Fixable Viability Dye eFluor™ 780 (Invitrogen) and anti-Lineage Cocktail 1 (Lin 1, CD3, CD14, CD16, CD19, CD20, CD56) from Biosciences. For the cytokines staining, cells were stimulated by the Cell Activation Cocktail (with Brefeldin A, Biolegend) for 3 h before surface staining. Then cells were pre-incubated with Fc Block (2 μl in 100 μl of cell suspension, BD Biosciences) for 10 min, Fixable Viability Dye (Invitrogen), and conjugated fluorescent primary antibodies were added for 30–45 min on ice in the dark. For intracellular staining, cells were fixed and permeated following the instruction (BD Biosciences). The compensation beads (Invitrogen) and cells with single fluorochrome and FMO controls were used as controls. Staining cells were analyzed with the BD flow cytometer (BD LSR II, BD Biosciences), and data was analyzed using FlowJo software V10.08 (Tree Star, OR, USA).

Live/dead staining, apoptosis and cytotoxicity analysis

Following MPDO incubation with αPD-1 or co-cultured with TILs (the ratio of TILs: cells in organoid was 5:1), the live or dead cells were measured by ViaStain AOPI Staining Solution (Nexcelom, CS2-0106), which was dual labeled AO (live cells, green) and PI (dead cells, red). The images were captured using a Zeiss LSM 710 (Carl Zeiss) and analyzed using the ZEN software. Live and dead cell quantitation were measured by the ratio of each dye to the total cell area.[28]

Apoptosis was measured after organoids were incubated with αPD-1 for 3 days. Organoids in Matrigel were washed with cold PBS to remove the Matrigel and digested using TrypLE Express (Gibco). Organoids in collagen gel were dissociated using collagenase IV to obtain a single-cell suspension. The single cells were washed with cold PBS twice and resuspended in 100 μl Annexin V Binding Buffer, subsequently stained with 5 μl of AV-FITC and 5 μl of 7-AAD solution (FITC Annexin V Apoptosis Detection Kit, Biolegend) for 15 min.[24,29]

TIL cytotoxicity was performed using the CytoTox 96® Non-Radioactive Cytotoxicity Assay. The organoids (cell number approximately 4×10^4) were cultured in 96 well-plate, and 2×10^5 TILs were added and co-cultured with organoids for 24 h. The lactate dehydrogenase (LDH) activity released by organoids was measured, and 4 replicates were used.

Small molecule screening

For a proof-of-concept screening assay, 12 compounds were selected to test the cell viability of organoids, including AZD8186, Copanlisib, Navitoclax, Dasatinib, Palbociclib, Seliciclib, Talazoparib, Entinostat, AMD3100, SB265610, Rogaratinib, GW2580, and DMSO control. The single cells were seeded onto Matrigel in the 96-well plates (5×10^3 cells per well) to grow four days for organoids generation. The compounds were diluted in a culture medium in a range of concentrations to incubate with organoids for four days. The cell viability was assayed using a cck-8 kit according to the manufacturer's protocol.

To measure whether these compounds enhance the cytotoxicity of TILs against organoids, the compounds (1 μM) were pre-incubated with organoids in Matrigel for 24 h, and then 2×10^5 TILs were added and co-cultured with organoids for 24 h. The LDH activity released by organoids was measured, and 4 replicates were used.[30,31] All the reagents and their sources are listed in the Table S2.

Statistical analysis

Data were analyzed by GraphPad Prism version 8 and depicted as mean ± SD. Statistical analysis was performed using a two-tailed Student's t-test and one-way ANOVA with a post-hoc Tukey test. p values < 0.05 were considered significant differences between groups; significance values are indicated as $*p < 0.05$, $**p < 0.01$.

Role of funders

The Funders had no roles in study design, data collection, analysis, interpretation, or decision to publish.

Results

MPDOs mimic parental tumor characteristics

We obtained 30 freshly resected melanoma tissues from patients. Single-cell suspension from the fresh tissues was cultured in Matrigel or collagen gel as previously reported[32–35] and supplemented with R-spondin 1, Noggin, WNT3A, EGF, and FGF.[36–38] The morphology of organoids in collagen gel or Matrigel was similar (Fig. 1a). Each MPDO was passaged at least once to confirm cell viability and organoid-forming capacity. An overall 73% (22/30) success rate was achieved. Spontaneous or treatment-induced tumor necrosis is very common in melanoma. We found that tumor tissues containing extensively necrotic tumors were less likely to give rise to MPDOs. Partially necrotic tumors might still generate MPDOs as necrotic tumor cells were gradually removed during serial passages. A majority of MPDOs (17/22) could continuously grow over 1 month and maintain complex stroma. The diameter of MPDOs was measured over time (Fig. 1a and b). 76% of the MPDOs (16/22) could passage several times after cryopreservation either in Matrigel or collagen gel (Fig. S1a).

The parental melanoma samples' tumor stages and mutation status are presented in Fig. 1c. Mutation of

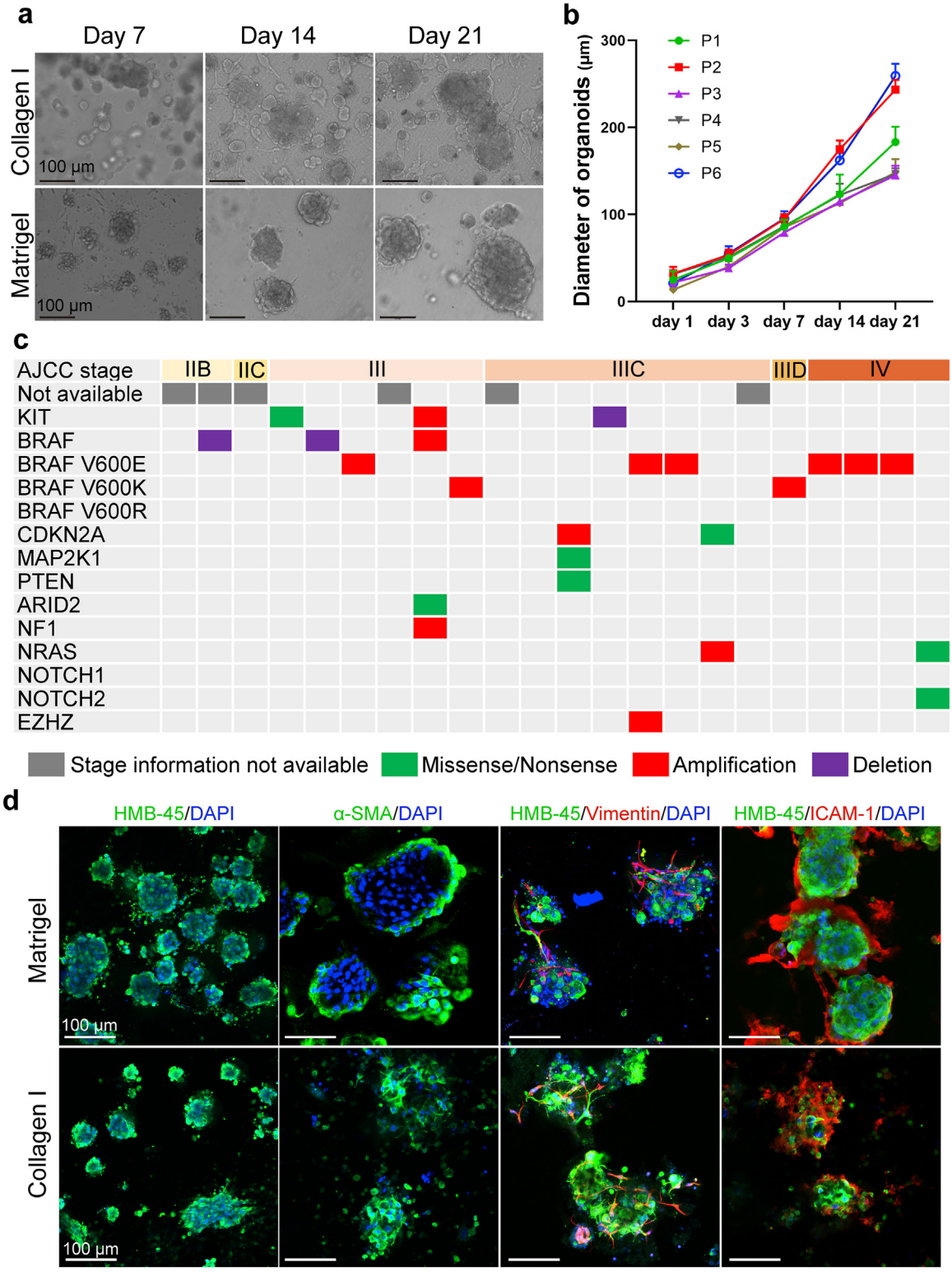

Fig. 1: **Melanoma patient-derived organoids (MPDOs) recapitulate parental tumor characteristics**. (**a**). Representative phase contrast images of MPDOs inlaid in Matrigel or embedded in collagen gel with time. These MPDOs were allowed to grow for 21 days without passaging. Scale bar, 100 μm. (**b**). Size of MPDOs (diameter) in Matrigel gel was measured over time. n = 3. (**c**). Tumor TNM stages and mutation status of

parental melanoma was analyzed by targeted next-generation sequencing at Penn Center for Personalized Diagnostics. Melanoma mutation status does not correlate with MPDO formation capacity.

To characterize the cellular components and stroma in MPDOs, we performed immunofluorescence stains using HMB-45, α-SMA, vimentin, and intercellular adhesion molecule 1 (ICAM-1). As the MPDOs were inlaid in the Matrigel, whole mount staining without sectioning was used for staining. In contrast, organoids in collagen gel were sectioned into 25 μm-sections and stained. Both methods revealed similar cellular components, but the morphology differed slightly, likely due to sectioning-induced changes (Fig. 1d and Fig. S1b). MPDOs preserved tumor stroma, including fibroblasts expressing α-SMA, mesenchymal cells expressing vimentin, and ICAM-1 that is involved in intercellular adhesion,[39,40] and T cell adhesion and migration.[41]

MPDOs preserve diverse immune cell components

To characterize the immune milieu in MPDOs, MPDOs cultured in the Matrigel, or collagen gel were stained with different immune cell markers or digested into a single-cell suspension for FACS analysis. Flow cytometric analysis demonstrated $CD45^+$, $CD4^+$, $CD8^+$, $CD14^+$, $CD15^+$, and $CD11b^+$ cells were present in the MPDOs from all 17 patients examined (Fig. 2 and Fig. S2). $CD45^+$ leucocytes ranged from 10 to 40% of all the live cells in the MPDOs and showed significant inter-tumoral heterogeneity (Fig. 2a). The percentage of $CD4^+$, $CD8^+$, $CD14^+$, $CD15^+$ cells, and other immune cells also varied in the MPDOs (Fig. 2b).

Regardless of whether the MPDOs were cultured in Matrigel or collagen gel, the percentages of immune cells were comparable to these in their corresponding parental tumor specimens after seven days (Fig. 2c). However, after one month of *in vitro* culture, all the immune cells in MPDOs significantly decreased (Fig. S3a).

Immunofluorescence stains confirmed that MPDOs contained various immune cells, including $CD45^+$, $CD3^+$, $CD8^+$, $CD14^+$, and $CD11b^+$ cells, which were interspersed with $HMB45^+$ tumor cells (Fig. 2d and Fig. S3b). These results confirmed that MPDOs retained diverse immune cell populations similar to those in the parental tumors after short-term culture.

MPDOs derived from melanoma tissue fragments

Previous reports have demonstrated that PDOs can be generated from small tumor fragments without mechanical or enzymatic dissociation into single cells, thereby preserving the local cytoarchitecture and cell–cell interactions of the original tumors.[26,28] To assess whether MPDOs could be generated from small melanoma fragments, we cut resected fresh tumor tissues into small fragments of approximately 500 μm in diameter using a surgical blade and cultured them in the organoid culturing medium. Tissue fragments from different areas of melanoma were cultured. Their morphology was shown in Fig. S4a. After 7–14 days of culture, some tissue fragments did not change in size or shape, and many of these tissue fragments were composed entirely of necrotic cells; while the tissue fragments containing viable tumor grow bigger (Fig. S4b). Some cells migrate out of the small tissue fragments during culture. The percentage of immune cells in different parts of the tumor varied, such as $CD45^+$, $CD3^+$, $CD8^+$, $CD14^+$, and $CD11b^+$ cells (Fig. S4c). The expression of α-SMA and vimentin also varied in different locations (Fig. S4c). As a result, MPDOs generated from small melanoma fragments were more heterogeneous, and some tissue fragments may contain only a few viable tumor cells, making it challenging to perform subsequent experiments.

MPDOs recapitulate immunosuppressive TME

Tumor cells execute immune evasion by upregulating programmed death-ligand 1 (PD-L1) expression.[42,43] PD-L1 is also expressed by multiple other cell types in the TME, such as cancer-associated fibroblasts (CAF),[43] tumor-associated macrophages (TAM), and other myeloid cells.[44,45] Indeed, many cells in the MPDOs were positive for PD-L1 by immunofluorescent staining (Fig. 3a). FACS analysis showed that PD-1 and CTLA-4 expression on $CD4^+$ and $CD8^+$ T cells in the MPDOs was similar to their parental tumors regardless of whether they were in Matrigel or collagen gel. PD-1 and CTLA-4 expression on Treg and PD-L1 expression on $CD11b^+$, $CD14^+$, $CD15^+$ myelomonocytic cells and $CD68^+$ macrophages were significantly higher in MPDOs cultured in Matrigel than their parental tumor tissues (Fig. 3b and Fig. S5a). Notably, the expression of PD-1 and PD-L1 on the immune cells in MPDOs significantly increased after 14 days of culture (Fig. 3c and Fig. S5b). These findings suggest that an immunosuppressive TME was maintained in MPDOs.

αPD-1 induce TIL expansion and increase tumor cell killing in MPDOs

We compared the expression of checkpoint proteins (PD-1, CTLA-4, TIM-3, and PD-L1) on $CD8^+$ T cells in parental

the parental melanoma samples. Targeted sequencing of the parental clinical samples was performed and single nucleotide variation (SNV) and copy number alterations (CNA) were reported. (**d**). Immunofluorescent stains of HMB-45, α-SMA, vimentin and ICAM-1 were performed on MPDOs cultured in Matrigel or collagen gel. The MPDOs inlaid in Matrigel were used as whole mount staining without section; while MPDOs embedded in collagen gel were sectioned into 25 μm slice and stained. Scale bar, 100 μm.

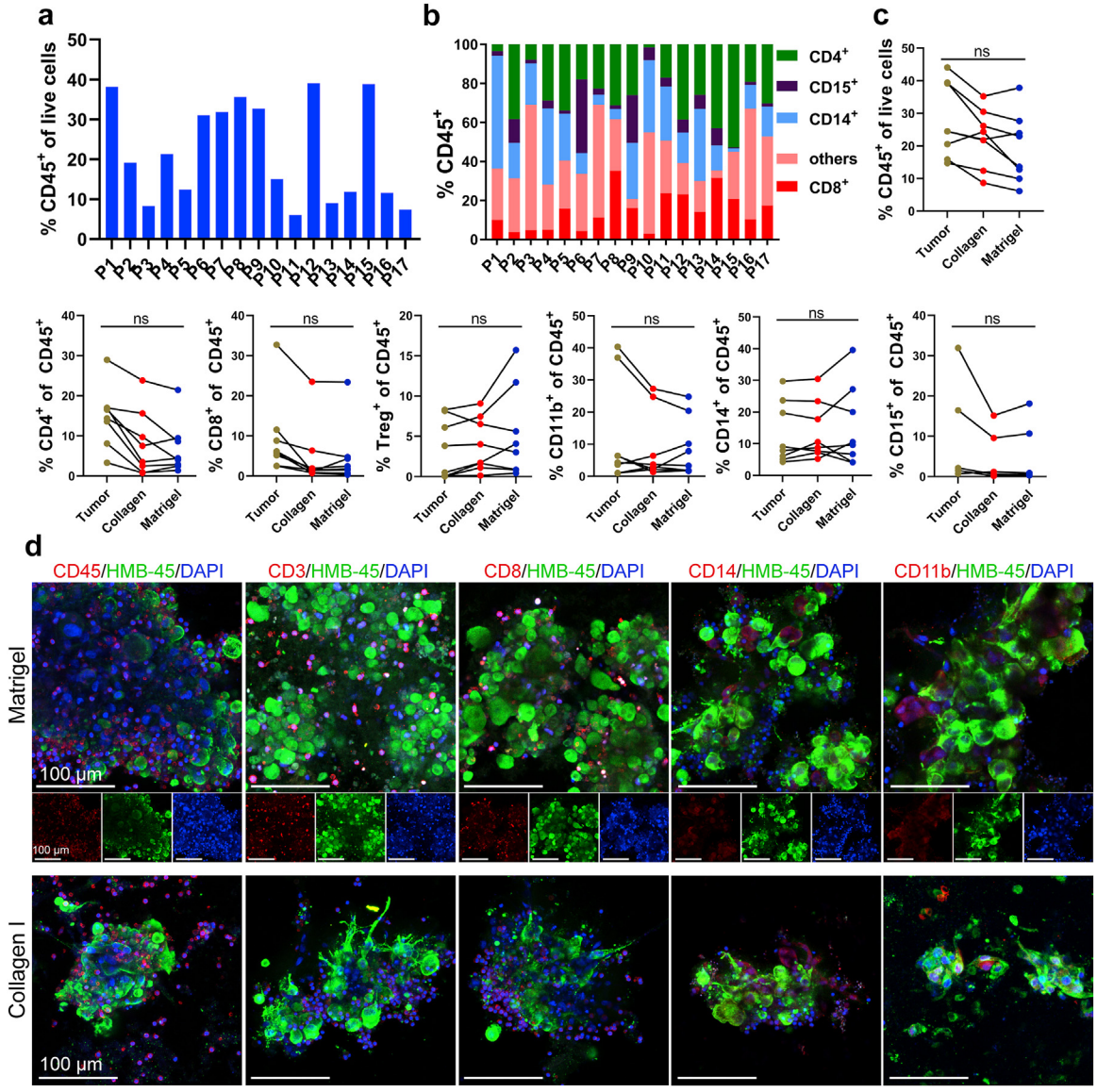

***Fig. 2:* MPDOs preserve diverse immune contexture**. (**a**). Quantification of CD45$^+$ leucocytes/live cells in MPDOs by FACS after culturing in Matrigel for 10 days. MPDOs from 17 melanoma patients were analyzed. (**b**). Immune cell composition in MPDOs, including CD4$^+$ T cells, CD8$^+$ T cells, CD14$^+$ cells, CD15$^+$ cells and other immune cells. MPDOs in Matrigel from 17 melanoma patients were analyzed. (**c**) Comparison of CD45$^+$, CD4$^+$, CD8$^+$, Treg$^+$, CD14$^+$, CD15$^+$ and CD11b$^+$ cells in parental tumors, MPDOs cultured in collagen gel or Matrigel after 7 days. n = 8. ns, no significance (nonparametric multiple test). (**d**). Representative immunofluorescent stains of CD45$^+$ leukocytes, CD3$^+$ T cells, CD8$^+$ T cells, CD14$^+$ monocytic cells and CD11b$^+$ myeloid cells in MPDOs cultured in collagen gel or Matrigel. Scale bar, 100 μm.

tumors with those on CD8$^+$ T cells in healthy donors' PBMCs. We found that levels of the checkpoint proteins were significantly higher (4–10 folds) in tumor-infiltrating CD8$^+$ T cells, as previously reported[46] (Fig. S6a).

Next, we tested whether αPD-1 (pembrolizumab) could expand CD8$^+$ T cells in MPDOs and whether IL-2 could enhance the effect. We established MPDOs in Matrigel using fresh melanomas from 11 different patients. Immunofluorescent staining revealed that the combination of αPD-1 and IL-2 significantly increased the number of CD3$^+$ T cells (3.9 times) and CD8$^+$ T cells (5.5 times) per organoid compared to the control (untreated group). Moreover, the combination of αPD-1 and IL-2 induced more T cell proliferation than αPD-1 alone (Fig. 4a). Interestingly, as the number of CD3$^+$ T cells and CD8$^+$ T cells expanded in MPDOs, the number of viable tumor cells decreased, resulting in smaller MPDOs.

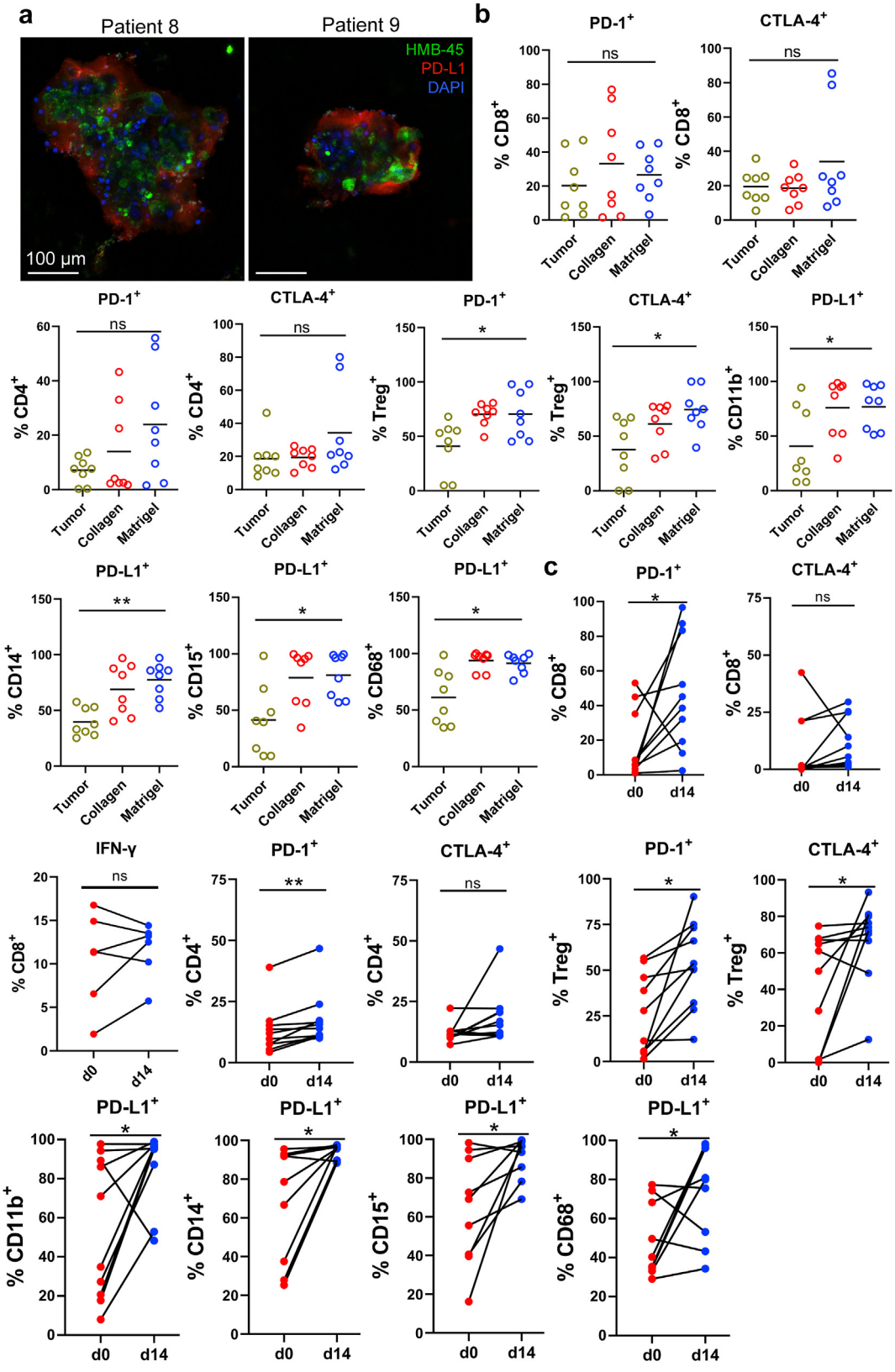
a
Patient 8
Patient 9
HMB-45
PD-L1
DAPI
100 μm
b
PD-1+
CTLA-4+
% CD8+
ns
Tumor
Collagen
Matrigel
% CD4+
% Treg+
% CD11b+
PD-L1+
% CD14+
% CD15+
% CD68+
c
d0
d14
IFN-γ
% CD8+

FACS analysis revealed that αPD-1 promoted $CD3^+$ and $CD8^+$ T cell proliferation in MPDOs from 5 to 6 of 11 patients, while αPD-1 plus IL-2 promoted $CD3^+$ and $CD8^+$ T cell proliferation in MPDOs from 9 of 11 patients, respectively (Fig. 4b). αPD-1 plus IL-2 treatment also expanded $CD4^+$ T cells, while no significant changes were seen in $CD45^+$ leukocytes in the MPDOs compared to the control or αPD-1 alone (Fig. S6b). The combination of αPD-1 plus IL-2 induced remarkable T cell proliferation ($CD3^+$, $CD4^+$, and $CD8^+$) up to 33-fold compared to the control in MPDOs (Fig. 4c). Interestingly, αPD-1 plus IL2 treatment decreased the ratio of $CD4^+$/$CD8^+$ T cells in the MPDOs with more increase of $CD8^+$ T cells (Fig. 4d). αPD-1 significantly decreased PD-1 levels in $CD8^+$ T cells, which might be resulted from Pembrolizumab may compete with the αPD-1 used in the FACS analysis or down-regulation of PD-1 expression in lymphocytes after Pembrolizumab treatment. However, αPD-1 plus IL2 treatment increased the proportion of $PD\text{-}1^+$ $CD8^+$ T cells and $TIM\text{-}3^+$ $CD8^+$ T cells compared to αPD-1 treatment alone (Fig. 4e). We performed cell killing and apoptosis assays using MPDOs from 3 random patients. αPD-1 plus IL2 treatment enhanced tumor cell death (Fig. 4f and Fig. S6c) and cell apoptosis in the MPDOs (Fig. 4g). However, we could not directly compare the response of MPDOs to αPD-1 and the corresponding melanoma clinical response to αPD-1 due to the small sample size and loss of follow-up of some patients.

Immunotherapy using TIL expanded by αPD-1 and IL-2

Even though adoptive cell therapy (ACT) with autologous TILs and high dose IL-2 following host lymphodepletion showed an objective response in melanoma patients,[47–49] there is still an unmet clinical need to improve the response rate and duration of TIL therapy. TILs are usually activated and expanded by IL2 and αCD3. However, induced T cell exhaustion can be seen in the TIL product.[50,51] We tested a new TIL expansion method using IL-2 and αPD-1 and compared it with conventional methods. We expanded TILs using tumor fragments from 14 patients with IL-2, αCD3, and/or αPD-1 for ten days. Different populations of immune cells, including $CD45^+$ leukocytes, $CD3^+$, $CD4^+$, and $CD8^+$ T cells, were measured (Fig. 5a and b and Fig. S7). IL-2, IL-2 plus αCD3, or IL-2 plus αPD-1 induced similar expansion of $CD45^+$, $CD3^+$, and $CD4^+$ T cells from tumor fragments (Fig. S7), however, TIL expanded using IL-2 plus αPD-1 yielded significantly more $CD8^+$ T cells (Fig. 5a and b). Significantly lower $PD\text{-}1^+$ or $PD\text{-}1^+$ $Tim\text{-}3^+$ expression on $CD8^+$ and $CD4^+$ T cells and more IFN-γ production were observed in $CD8^+$ T cells expanded by IL-2 plus αPD-1 compared to that of IL-2 or IL-2 plus αCD3 (Fig. 5b and Fig. S7), suggesting that presence of αPD-1 during TIL expansion may be helpful.

We tested TIL chemotaxis and migratory capacity using MPDOs embedded in the collagen gel. MPDOs and expanded TILs were from the same melanoma patient in these experiments. Cells in MPDOs were labeled with an orange dye (red) and embedded in the bottom of the collagen gel, while the expanded autochthonous TILs were labeled CFSE (green) and added to the top of the collagen gel. It has been shown that collagen gel matrices were suitable for observing TIL migration through extracellular matrix and stroma, miming *in vivo* conditions.[52] We observed that MPDOs attracted TIL migrating toward them (Fig. 5c). TILs expanded by IL-2 plus αPD-1 or IL-2 plus αCD3 demonstrated increased motility, as shown by time-lapse imaging compared to TILs expanded by IL-2 only (Fig. 5c). Furthermore, TIL infiltration was also studied using MPDOs that were inlaid in the Matrigel. TIL was labeled with CFSE (green), and cells in the MPDOs were labeled with orange dye (red). TILs expanded by IL-2 plus αPD-1 or IL-2 plus αCD3 showed more infiltration into MPDOs than IL-2 alone (Fig. 5d).

MPDOs inlaid in the Matrigel were used to assess TIL-tumor killing. Expanded autochthonous TILs from 3 different melanoma patients were used in the cytotoxicity assessment studies. The expanded TIL cell number, percentage of $CD3^+$ and $CD8^+$ T cells, and checkpoint protein expression on TILs varied depending on the patients, but the viability of TILs was similar (Fig. 6a and b). Live/dead cell staining revealed that TIL expanded by IL-2 plus αPD-1 or IL-2 plus αCD3 killed significantly more cells in the MPDOs than IL-2 alone (Fig. 6c). LDH release assays showed that TILs expanded by IL-2 plus αPD-1 exhibited better cytotoxicity against MPDOs than IL-2 alone or IL-2 plus αCD3 in three patients (Fig. 6d). These results suggest that TIL expanded by IL-2 plus αPD-1 may infiltrate MPDOs better and/or have better cellular function than the conventional methods.

Small molecule screen to identify compounds that enhance TIL function

Due to the high preservation of genetic and epigenetic variations in patients, PDOs have been used for small

Fig. 3: **Immunosuppressive TME in MPDOs**. (**a**). Representative immunofluorescent staining of PD-L1 in MPDOs cultured in Matrigel from 2 patients (patients 8 and 9). Scale bar, 100 μm. (**b**). PD-1 and CTLA-4 expression on $CD4^+$, $CD8^+$ T cells and $Treg^+$ cells, and PD-L1 expression on $CD11b^+$, $CD14^+$, $CD15^+$ and $CD68^+$ immune cells by FACS analysis. n = 8. $^*p < 0.05$ (nonparametric multiple test); ns, no significance. (**c**). PD-1, CTLA-4, PD-L1 and IFN-γ expression on immune cells in MPDOs cultured in Matrigel at day 0 and day 14. Day 0: single cell suspension of tumor tissue before culture. Day 14: MPDOs were cultured in Matrigel for 14 days. n = 10. $^*p < 0.05$ (paired Student's t test).

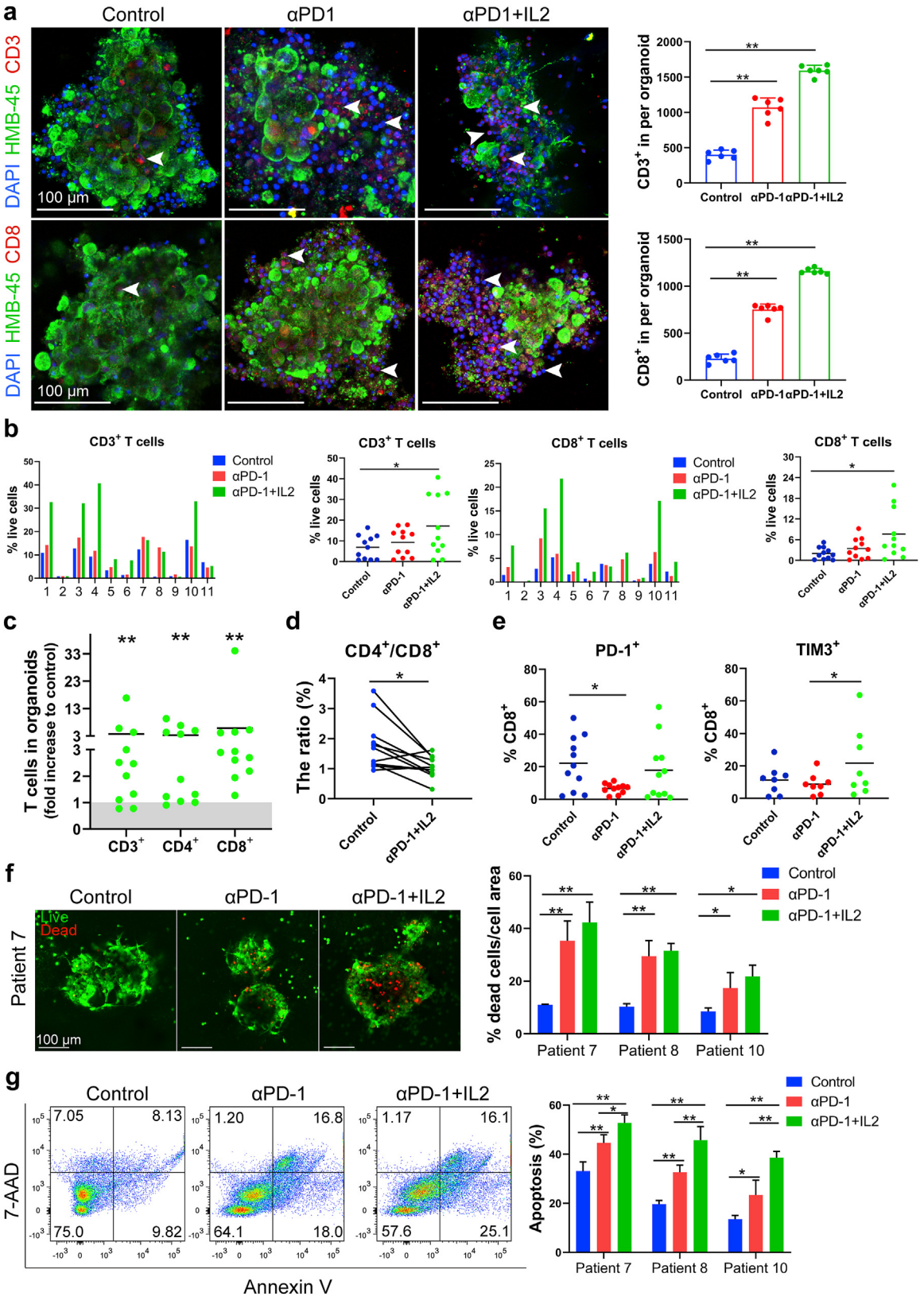
a
Control
αPD1
αPD1+IL2
DAPI HMB-45 CD3
DAPI HMB-45 CD8
100 μm
CD3+ in per organoid
CD8+ in per organoid
Control αPD-1 αPD-1+IL2
b
CD3+ T cells
CD8+ T cells
% live cells
Control
αPD-1
αPD-1+IL2
c
T cells in organoids (fold increase to control)
CD3+ CD4+ CD8+
d
CD4+/CD8+
The ratio (%)
e
PD-1+
TIM3+
% CD8+
f
Patient 7
Live
Dead
% dead cells/cell area
Patient 7 Patient 8 Patient 10
g
7-AAD
Annexin V
7.05 8.13 75.0 9.82
1.20 16.8 64.1 18.0
1.17 16.1 57.6 25.1
Apoptosis (%)

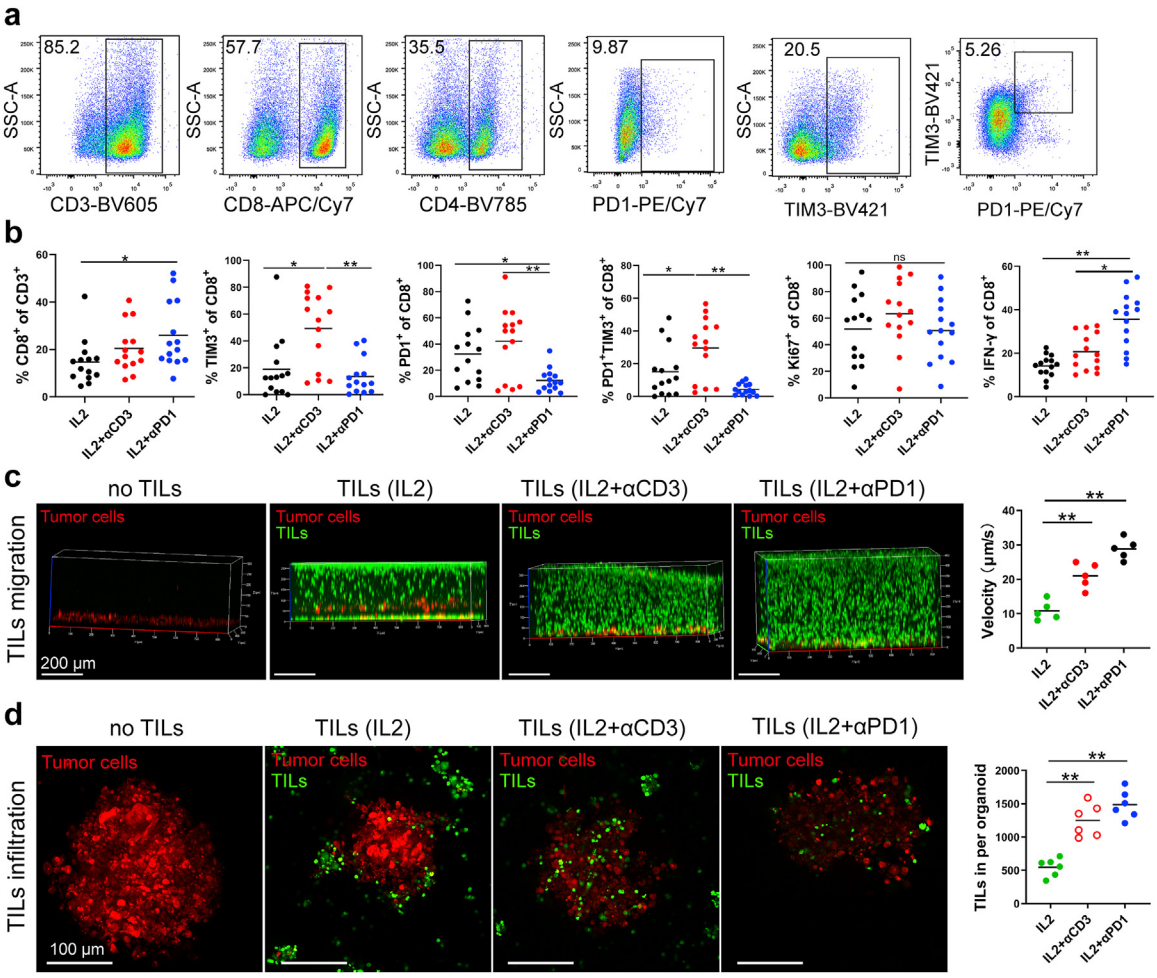

Fig. 5: **TIL migration and infiltration toward MPDOs**. (**a**). Representative FACS Scatter plots of $CD3^+$, $CD4^+$, $CD8^+$ and the expression of PD-1 and TIM-3 after TIL expansion from tumor fragments of 14 patients by IL2 or IL2 plus αCD3/αPD-1. (**b**). Quantification of $CD8^+$ T cells, PD-1, TIM-3, Ki-67 and IFN-γ expression on $CD8^+$ T cells after TIL expansion by FACS. n = 14, $^*p < 0.05$, $^{**}p < 0.01$ (nonparametric multiple test). (**c**). Snapshots of autochthonous TIL migration toward MPDOs, Time-lapse images of the movement of TILs were captured by confocal microscopy. Imaging was performed within 24 h after TILs were added onto the top of collagen gel and the velocity of TILs was quantified. $^*p < 0.05$ (nonparametric multiple test). MPDOs pre-labeled with orange dye (red) were embedded in the bottom of the collagen gel and TILs pre-labeled with CFSE (green) were added onto the top of the collagen gel. (**d**). Snapshots of autochthonous TILs infiltrating into MPDOs were performed by microscopy after TILs and MPDOs co-culture, and the TILs per organoid were calculated. MPDOs pre-labeled with orange dye were inlaid in Matrigel and TILs pre-labeled with CFSE. IL2: TILs expanded by IL2 (600 IU/ml); IL2 + αCD3: IL2 (600 IU/ml) plus αCD3 (2 μg/ml); IL2 + αPD-1: IL2 (600 IU/ml) plus αPD-1 (100 μg/ml). Scale bar, 100 μm $^{**}p < 0.01$ (nonparametric multiple test).

Fig. 4: **αPD-1 and IL-2 reinvigorate $CD8^+$ T cells in MPDOs**. (**a**). Representative immunofluorescent images and quantification of $CD3^+$ T cells and $CD8^+$ T cells in MPDOs cultured in Matrigel after IL2 and αPD-1 treatment. Scale bar, 100 μm. White arrow heads point to $CD3^+$ or $CD8^+$ T cells. $^*p < 0.05$; $^{**}p < 0.01$ (nonparametric multiple test). (**b**). FACS analysis of $CD3^+$ and $CD8^+$ cells in MPDOs cultured in Matrigel from 11 melanoma patients after IL2 and αPD-1 treatment. $^*p < 0.05$ (nonparametric multiple test). (**c**). Fold changes of $CD3^+$, $CD4^+$ and $CD8^+$ cells in MPDOs in Matrigel from 11 melanoma patients after treated with IL2 and αPD-1. (**d**). Comparison of $CD4^+/CD8^+$ ratio in MPDOs with or without IL2 and αPD-1 treatment. (**e**). FACS analysis of PD-1 and TIM-3 expression in MPDOs in Matrigel from 11 patients after IL2 and αPD-1 treatment. n = 11, $^*p < 0.05$; ns, no significance. (**f**). Live/dead cell staining of MPDOs in Matrigel and the quantitation of dead cells within MPDOs after IL2 and αPD-1 treatment. MPDOs from 3 patients were tested. Scale bar, 100 μm. n = 3, $^*p < 0.05$ (nonparametric multiple test); ns, no significance. (**g**). Annexin V and 7-AAD staining of tumor cell death within MPDOs in Matrigel after IL2 and αPD-1 treatment. Quantitation of apoptotic cells within MPDOs from 3 patients was shown.

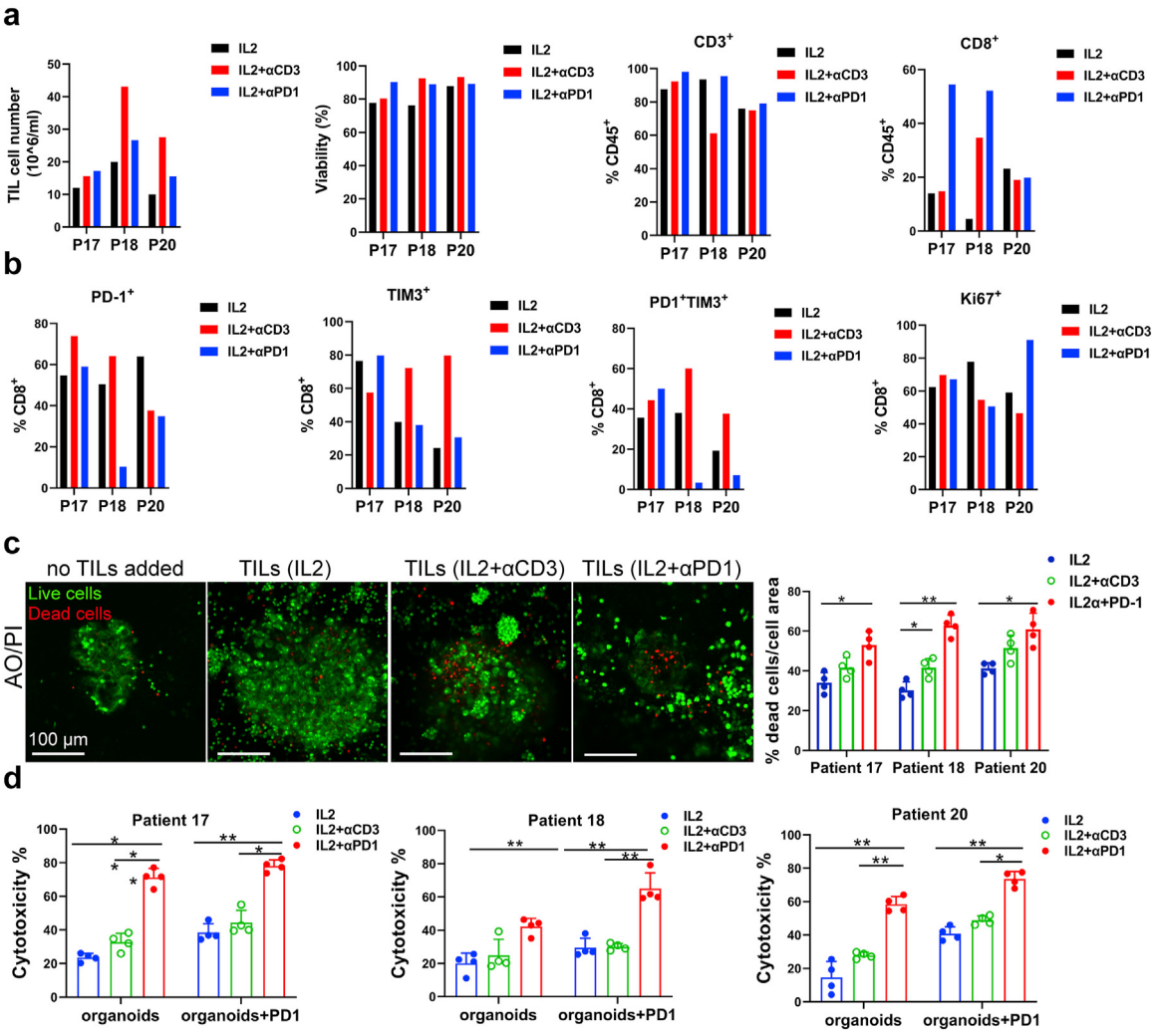

Fig. 6: **Autochthonous TIL immunotherapy using MPDOs**. (**a**). Expanded TILs used for cytotoxicity assessment from 3 patients. Cell number, viability and percentage of $CD3^+$ and $CD8^+$ cells in TILs were measured by FACS. (**b**). PD-1, TIM-3 and Ki-67 expression on $CD8^+$ T cells were measured by FACS after TIL expansion from 3 patients. (**c**). Live (AO = green)/dead (PI = red) images and quantification of MPDOs inlaid in Matrigel after co-culture with autochthonous TILs for 24 h. Scale bar, 100 μm. (**d**). Cytotoxicity of autochthonous TILs from 3 patients against MPDOs in Matrigel was detected using the LDH release assay. IL2: TILs expanded by IL2 (600 IU/ml); IL2 + αCD3: IL2 (600 IU/ml) plus αCD3 (2 μg/ml); IL2 + αPD-1: IL2 (600 IU/ml) plus αPD-1 (100 μg/ml). $^*p < 0.05$, $^{**}p < 0.01$ (nonparametric multiple test).

molecule screens.[14,25,34,35] To identify compounds that may enhance the therapeutic efficacy of TIL therapy. We perform a small-scale screening using PI3K inhibitor (AZD8186, Copanlisib), Bcl-xl inhibitor (Navitoclax), BCR-ABL antagonist (Dasatinib), CDK inhibitor (Palbociclib, Seliciclib), PARP inhibitor (Talazoparib), HDAC inhibitor (Entinostat), CXCR4 inhibitor (AMD3100), CXCR2 inhibitor (SB265610), FGFR inhibitor (Rogaratinib) and CSF-1R inhibitor (GW2580).

We performed a dose–response study using these compounds in MPDOs cultured in Matrigel from three patients. 5×10^3 single cells from digested tumor tissues per well were seeded in Matrigel in a 96-well plate for four days. After organoids were visually apparent, different compounds were added to the culture medium. The cck-8 assay measured MPDO viability after treatment with varying concentrations of compounds (0.01, 0.1, 1, and 10 μM) for four days (Fig. 7a). These compounds inhibited the viability of cells in the MPDOs at a concentration equal to or higher than 1 μM (Fig. 7a). Inter-tumoral heterogeneity was apparent as MPDOs from different patients responded differently to these compounds. Copanlisib and Palbociclib showed better anti-tumor efficacy than other compounds.

Next, we studied whether these compounds could enhance the cytotoxicity of autochthonous TILs. After

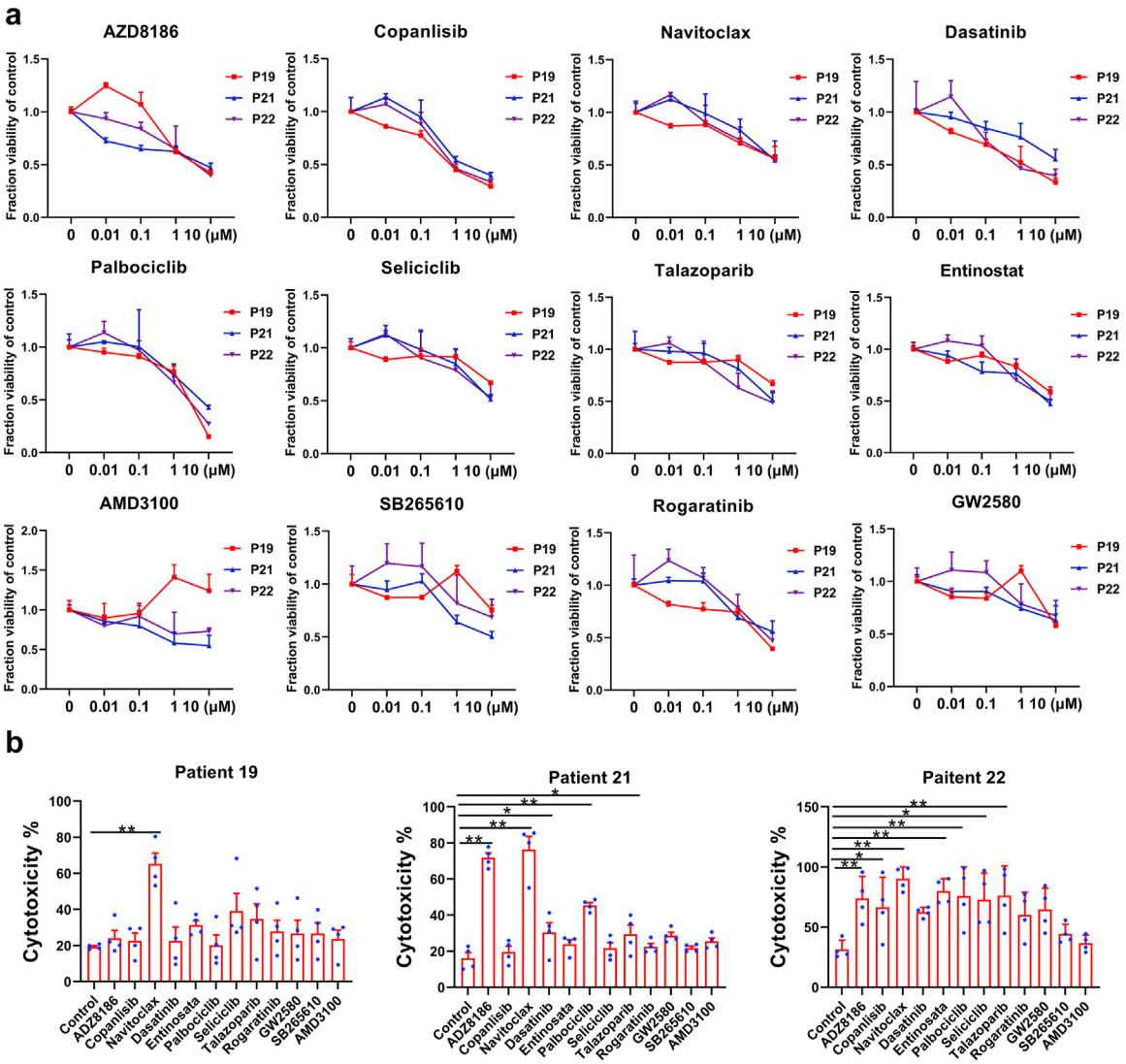

Fig. 7: **Small molecule screen using MPDOs**. (**a**). Dose–response curves of PI3K inhibitor (AZD8186, Copanlisib), Bcl-xl inhibitor (Navitoclax), BCR-ABL antagonist (Dasatinib), CDK inhibitor (Palbociclib, Seliciclib), PARP inhibitor (Talazoparib), HDAC inhibitor (Entinostat), CXCR4 inhibitor (AMD3100), CXCR2 inhibitor (SB265610), FGFR inhibitor (Rogaratinib) and CSF-1R inhibitor (GW2580) against MPDOs in Matrigel. The viability of MPDOs was detected by the CCK-8 kit. MPDOs from 3 melanoma patients were used. (**b**). Cytotoxicity of autochthonous TILs against MPDOs after addition of small molecules were measured using the LDH release assay. Autochthonous TILs from 3 patients were used. n = 3, $^{*}p < 0.05$, $^{**}p < 0.01$ (nonparametric multiple test).

the compounds (1 μM) were pre-incubated with MPDOs for 24 h, 2×10^5 autochthonous TILs were co-cultured with MPDOs in Matrigel for an additional 24 h. We discovered that Navitoclax enhanced the cytotoxicity of TIL against MPDOs in 3 of 3 patients; while AZD8186, Palbociclib and Talazoparib enhanced the cytotoxicity of TIL against MPDOs in 2 of 3 patients (Fig. 7b).

Discussion

We explored two different approaches for producing MPDOs and discovered that the immune cell makeup and morphology of MPDOs strongly resemble those of their primary tumors, regardless of the embedding technique employed. The TME in MPDOs exhibited a highly immunosuppressive profile, similar to their parental tumors. A subset of $CD8^+$ T cells in the MPDOs showed exhausted phenotypes that could be reinvigorated with αPD-1. TILs that were expanded with IL-2 plus αPD-1 displayed superior chemotaxis and cytotoxicity toward melanoma compared to other expansion methods. We also found that navitoclax enhanced TIL cytotoxicity against MPDOs. These findings support the

use of MPDOs as a tool for evaluating the effectiveness of TIL therapy and checkpoint blockade (Fig. 8).

To generate ideal PDOs, it is crucial to maintain the cellular components and tumor structure of their parental tumors to capture the complexity and heterogeneity of cancer. While the culture of tissue fragments can provide native stromal and immune components,[26] this method may not be suitable for some cancers, particularly those with excessive tumor necrosis. MPDOs generated from dissociated melanoma tissue are more suitable, especially when the fresh tissue is partially necrotic. Furthermore, the choice of the matrix in which to culture the MPDOs can impact subsequent assays. For instance, MPDOs in collagen gel matrices are appropriate for studying chemotaxis and migration of TIL through the extracellular matrix and stroma,[52] while MPDOs inlaid in Matrigel are ideal for assessing TIL-tumor cell contact and direct killing by TILs.

MPDOs exhibit significant intertumoral variation in immune cell infiltrate, similar to their parental tumors. We observe diverse immune cells such as $CD4^+$, $CD8^+$, Treg, $CD14^+$, $CD15^+$, and $CD11b^+$ cells in MPDOs. TAM and other myeloid cells play critical roles in tumor immune evasion.[53,54] These cells in MPDOs also express high levels of PD-L1, recapitulating their immunosuppressive role in the tumor tissues. Interestingly, PD-1 and CTLA-4 on T cells and PD-L1 expression on myeloid cells are increased in the MPDOs after culturing for two weeks, supporting that the immunosuppressive TME is maintained in the culture conditions. However, similar to the prior studies, resident immune cells in the MPDOs have a limited lifespan and decline gradually even when supplied with IL-2 and other cytokines.[24,28] Thus, MPDOs are best used after short-term culture. Nevertheless, we find that cells from early passage MPDOs can be frozen/thawed and used for MPDO generation at a later time.

MPDOs retain diverse immune components and may provide a real-time platform to test ICB therapy response *in vitro*. Similar to the clinical responses to PD-1 blockade,[55,56] we find tumor-infiltrating $CD8^+$ T cells in MPDOs can be expanded by αPD-1. However, $CD8^+$ T cell expansion only occurred in MPDOs from approximately 45% of melanoma patients. This inter-tumoral heterogeneity may reflect melanoma patients' αPD-1 clinical response rates.[57,58] We demonstrate that IL-2 increases T cell expansion in the MPDOs, but it also increases checkpoint protein expression in the immune cells. MPDO response to αPD-1 may potentially reflect parental tumor response to αPD-1 clinically. However,

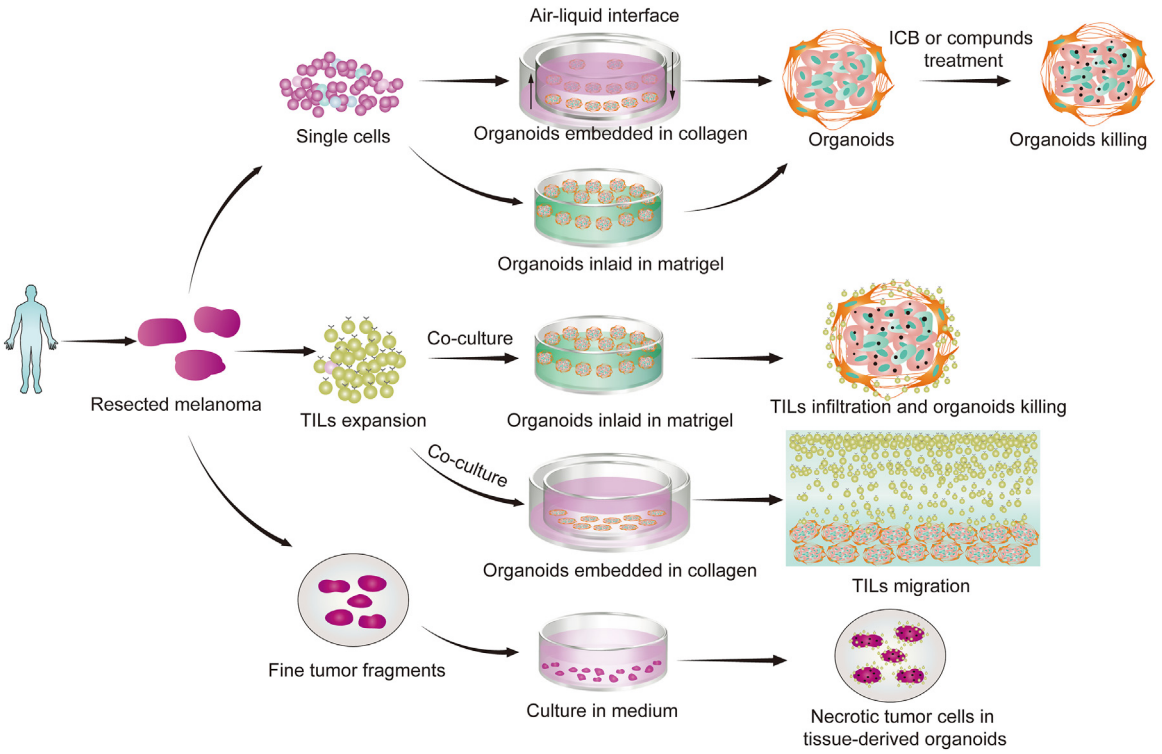

Fig. 8: Two different MPDOs (in collagen gel or in Matrigel) maintain many key features of human melanoma tissues and sustain highly immunosuppressive tumor microenvironment. MPDOs in Matrigel are used to assess cytotoxicity of various treatments and MPDOs in collagen gel are used to evaluate migratory capacity of TILs. The use of these culture systems may thus provide a powerful approach to develop personalized immunotherapy.

our ability to conclude the correlation between the response of MPDOs to αPD-1 and the corresponding melanoma clinical response to αPD-1 is limited by the small sample size and loss of follow-up of some patients.

We discover that TILs expanded from tumor fragments using IL-2 and αPD-1 have better quality than TILs expanded using IL2 alone or IL2 plus αCD3. The expansion efficiency and ratio varied in different patients. $CD8^+$ T cells expanded using IL-2 and αPD-1 show significantly lower expression of TIM-3 and higher expression of IFN-γ. TILs expanded by IL-2 and αPD-1 show better chemotaxis and migration to tumor cells, and infiltrate and kill tumor cells in the MPDOs more effectively than TIL expanded using other methods. Thus, MPDOs can be used to test the efficacy of autologous TILs in melanoma. Our data support that the addition of αPD-1 during TIL expansion may enhance their functions. Our small molecule screen assay discovered that Navitoclax enhances melanoma killing efficacy of TILs. These data suggest that the treatment efficacy of TILs may be improved by combining them with a small molecule inhibitor.

In summary, MPDOs effectively preserve essential characteristics of human melanoma tissues and sustain a highly immunosuppressive TME. These features make them valuable tools not only for studying the interaction of tumor cells with immune cells but also for modeling TME-intrinsic immune cell responses to checkpoint blockade, TIL therapy, and small molecule targeted therapy. Using these culture systems may thus provide a powerful approach to develop personalized immunotherapy and design combination therapies for clinical-translational efforts in precision medicine.

Contributors

X.X and L.O designed the experiments and interpreted the data. L.O and S.L conducted experiments and developed methodologies. X.X, L.O, H.W, S.L, R.L, D.E, A.C.H, G.K, J.M, T.M, L.S, R.A, and A.F. managed patient melanoma samples, L.O, Y.G, R.L, and L.G acquired experimental data. X.X and L.O wrote the manuscript. H.M, W.G, A.C.H, J.K, Q.C, B.T, Y.F, D.E, and M.H, provided administrative, technical, or material support. L.O and X.X have accessed and verified the underlying data, and X.X and L.O were responsible for the decision to submit the manuscript. Every author approved the manuscript.

Data sharing statement

All primary data associated with this study are available upon request to the corresponding author for individuals with appropriate data-sharing agreements in place. All the data related to this study are present in the paper or Supplementary Materials.

Declaration of interests

Giorgos Karakousis served as an advisory board member and received clinical trial support from Merck. Other authors declare that they have no competing interests.

Acknowledgment

This work was supported by the NIH grants CA114046, CA261608, CA258113, and the Tara Miller melanoma foundation. The authors thank the Tumor Tissue and Biospecimen Bank at Penn for assisting with tissue collection.

Appendix A. Supplementary data

Supplementary data related to this article can be found at https://doi.org/10.1016/j.ebiom.2023.104614.

References

1 Keung EZ, Gershenwald JE. The eighth edition American Joint Committee on Cancer (AJCC) melanoma staging system: implications for melanoma treatment and care. *Expert Rev Anticancer Ther*. 2018;18(8):775–784.
2 Ascierto PA, Flaherty K, Goff S. Emerging strategies in systemic therapy for the treatment of melanoma. *Am Soc Clin Oncol Educ Book*. 2018;38:751–758.
3 Silva IP, Long GV. Systemic therapy in advanced melanoma: integrating targeted therapy and immunotherapy into clinical practice. *Curr Opin Oncol*. 2017;29(6):484–492.
4 Shannan B, Perego M, Somasundaram R, Herlyn M. Heterogeneity in melanoma. *Cancer Treat Res*. 2016;167:1–15.
5 Mak IW, Evaniew N, Ghert M. Lost in translation: animal models and clinical trials in cancer treatment. *Am J Transl Res*. 2014;6(2):114–118.
6 Patrizii M, Bartucci M, Pine SR, Sabaawy HE. Utility of glioblastoma patient-derived orthotopic xenografts in drug discovery and personalized therapy. *Front Oncol*. 2018;8:23.
7 Tentler JJ, Tan AC, Weekes CD, et al. Patient-derived tumour xenografts as models for oncology drug development. *Nat Rev Clin Oncol*. 2012;9(6):338–350.
8 Smalley KS, Haass NK, Brafford PA, Lioni M, Flaherty KT, Herlyn M. Multiple signaling pathways must be targeted to overcome drug resistance in cell lines derived from melanoma metastases. *Mol Cancer Ther*. 2006;5(5):1136–1144.
9 Shannan B, Chen Q, Watters A, et al. Enhancing the evaluation of PI3K inhibitors through 3D melanoma models. *Pigment Cell Melanoma Res*. 2016;29(3):317–328.
10 Marsavela G, Aya-Bonilla CA, Warkiani ME, Gray ES, Ziman M. Melanoma circulating tumor cells: benefits and challenges required for clinical application. *Cancer Lett*. 2018;424:1–8.
11 Pasca AM, Sloan SA, Clarke LE, et al. Functional cortical neurons and astrocytes from human pluripotent stem cells in 3D culture. *Nat Methods*. 2015;12(7):671–678.
12 Clevers H. Modeling development and disease with organoids. *Cell*. 2016;165(7):1586–1597.
13 Shi R, Radulovich N, Ng C, et al. Organoid cultures as preclinical models of non-small cell lung cancer. *Clin Cancer Res*. 2020;26(5):1162–1174.
14 van de Wetering M, Francies HE, Francis JM, et al. Prospective derivation of a living organoid biobank of colorectal cancer patients. *Cell*. 2015;161(4):933–945.
15 Ohlund D, Handly-Santana A, Biffi G, et al. Distinct populations of inflammatory fibroblasts and myofibroblasts in pancreatic cancer. *J Exp Med*. 2017;214(3):579–596.
16 Bein A, Shin W, Jalili-Firoozinezhad S, et al. Microfluidic organ-on-a-chip models of human intestine. *Cell Mol Gastroenterol Hepatol*. 2018;5(4):659–668.
17 Neal JT, Kuo CJ. Organoids as models for neoplastic transformation. *Annu Rev Pathol*. 2016;11(1):199–220.
18 Vlachogiannis G, Hedayat S, Vatsiou A, et al. Patient-derived organoids model treatment response of metastatic gastrointestinal cancers. *Science*. 2018;359(6378):920–926.
19 Seip K, Jørgensen K, Haselager MV, et al. Stroma-induced phenotypic plasticity offers phenotype-specific targeting to improve melanoma treatment. *Cancer Lett*. 2018;439:1–13.
20 Klemm F, Joyce JA. Microenvironmental regulation of therapeutic response in cancer. *Trends Cell Biol*. 2015;25(4):198–213.
21 Quail DF, Joyce JA. Microenvironmental regulation of tumor progression and metastasis. *Nat Med*. 2013;19(11):1423–1437.
22 Vilgelm AE, Bergdorf K, Wolf M, et al. Fine-needle aspiration-based patient-derived cancer organoids. *iScience*. 2020;23(8):101408.
23 Rosenberg SA, Restifo NP. Adoptive cell transfer as personalized immunotherapy for human cancer. *Science*. 2015;348(6230):62–68.
24 Neal JT, Li X, Zhu J, et al. Organoid modeling of the tumor immune microenvironment. *Cell*. 2018;175(7):1972–1988.e16.
25 Huang L, Holtzinger A, Jagan I, et al. Ductal pancreatic cancer modeling and drug screening using human pluripotent stem cell- and patient-derived tumor organoids. *Nat Med*. 2015;21(11):1364–1371.

26 Jacob F, Salinas RD, Zhang DY, et al. A patient-derived glioblastoma organoid model and biobank recapitulates inter- and intratumoral heterogeneity. *Cell*. 2020;180(1):188–204.e22.
27 Lu YC, Jia L, Zheng Z, Tran E, Robbins PF, Rosenberg SA. Single-cell transcriptome analysis reveals gene signatures associated with T-cell persistence following adoptive cell therapy. *Cancer Immunol Res*. 2019;7(11):1824–1836.
28 Jenkins RW, Aref AR, Lizotte PH, et al. Ex vivo profiling of PD-1 blockade using organotypic tumor spheroids. *Cancer Discov*. 2018;8(2):196–215.
29 Shivange G, Urbanek K, Przanowski P, et al. A single-agent dual-specificity targeting of FOLR1 and DR5 as an effective strategy for ovarian cancer. *Cancer Cell*. 2018;34(2):331–345.e11.
30 Stein A, Simnica D, Schultheiß C, et al. PD-L1 targeting and subclonal immune escape mediated by PD-L1 mutations in metastatic colorectal cancer. *J Immunother Cancer*. 2021;9(7):e002844.
31 Xia C, Liu C, He Z, Cai Y, Chen J. Metformin inhibits cervical cancer cell proliferation by modulating PI3K/Akt-induced major histocompatibility complex class I-related chain A gene expression. *J Exp Clin Cancer Res*. 2020;39(1):127.
32 Huang W, Navarro-Serer B, Jeong YJ, et al. Pattern of invasion in human pancreatic cancer organoids is associated with loss of SMAD4 and clinical outcome. *Cancer Res*. 2020;80(13):2804–2817.
33 Buchmann B, Engelbrecht LK, Fernandez P, et al. Mechanical plasticity of collagen directs branch elongation in human mammary gland organoids. *Nat Commun*. 2021;12(1):2759.
34 Kim M, Mun H, Sung CO, et al. Patient-derived lung cancer organoids as in vitro cancer models for therapeutic screening. *Nat Commun*. 2019;10(1):3991.
35 Pauli C, Hopkins BD, Prandi D, et al. Personalized in vitro and in vivo cancer models to guide precision medicine. *Cancer Discov*. 2017;7(5):462–477.
36 Boj SF, Hwang CI, Baker LA, et al. Organoid models of human and mouse ductal pancreatic cancer. *Cell*. 2015;160(1-2):324–338.
37 Fujii M, Shimokawa M, Date S, et al. A colorectal tumor organoid library demonstrates progressive loss of niche factor requirements during tumorigenesis. *Cell Stem Cell*. 2016;18(6):827–838.
38 Boonekamp KE, Kretzschmar K, Wiener DJ, et al. Long-term expansion and differentiation of adult murine epidermal stem cells in 3D organoid cultures. *Proc Natl Acad Sci U S A*. 2019;116(29):14630–14638.
39 Yanguas A, Garasa S, Teijeira A, Auba C, Melero I, Rouzaut A. ICAM-1-LFA-1 dependent CD8+ T-lymphocyte aggregation in tumor tissue prevents recirculation to draining lymph nodes. *Front Immunol*. 2018;9:2084.
40 Krisp C, Parker R, Pascovici D, et al. Proteomic phenotyping of metastatic melanoma reveals putative signatures of MEK inhibitor response and prognosis. *Br J Cancer*. 2018;119(6):713–723.
41 Teijeira A, Hunter MC, Russo E, et al. T cell migration from inflamed skin to draining lymph nodes requires intralymphatic crawling supported by ICAM-1/LFA-1 interactions. *Cell Rep*. 2017;18(4):857–865.
42 Chen L, Han X. Anti-PD-1/PD-L1 therapy of human cancer: past, present, and future. *J Clin Invest*. 2015;125(9):3384–3391.
43 Taube JM, Klein A, Brahmer JR, et al. Association of PD-1, PD-1 ligands, and other features of the tumor immune microenvironment with response to anti-PD-1 therapy. *Clin Cancer Res*. 2014;20(19):5064–5074.
44 Prima V, Kaliberova LN, Kaliberov S, Curiel DT, Kusmartsev S. COX2/mPGES1/PGE2 pathway regulates PD-L1 expression in tumor-associated macrophages and myeloid-derived suppressor cells. *Proc Natl Acad Sci U S A*. 2017;114(5):1117–1122.
45 Topalian SL, Taube JM, Anders RA, Pardoll DM. Mechanism-driven biomarkers to guide immune checkpoint blockade in cancer therapy. *Nat Rev Cancer*. 2016;16(5):275–287.
46 Mohme M, Maire CL, Geumann U, et al. Local intracerebral immunomodulation using interleukin-expressing mesenchymal stem cells in glioblastoma. *Clin Cancer Res*. 2020;26(11):2626–2639.
47 Chandran SS, Somerville RPT, Yang JC, et al. Treatment of metastatic uveal melanoma with adoptive transfer of tumour-infiltrating lymphocytes: a single-centre, two-stage, single-arm, phase 2 study. *Lancet Oncol*. 2017;18(6):792–802.
48 Rosenberg SA, Yang JC, Sherry RM, et al. Durable complete responses in heavily pretreated patients with metastatic melanoma using T-cell transfer immunotherapy. *Clin Cancer Res*. 2011;17(13):4550–4557.
49 Wu R, Forget MA, Chacon J, et al. Adoptive T-cell therapy using autologous tumor-infiltrating lymphocytes for metastatic melanoma: current status and future outlook. *Cancer J*. 2012;18(2):160–175.
50 Giuffrida L, Sek K, Henderson MA, et al. IL-15 preconditioning augments CAR T cell responses to checkpoint blockade for improved treatment of solid tumors. *Mol Ther*. 2020;28(11):2379–2393.
51 Wang Y, Sun SN, Liu Q, et al. Autocrine complement inhibits IL10-dependent T-cell-mediated antitumor immunity to promote tumor progression. *Cancer Discov*. 2016;6(9):1022–1035.
52 Dangaj D, Bruand M, Grimm AJ, et al. Cooperation between constitutive and inducible chemokines enables T cell engraftment and immune attack in solid tumors. *Cancer Cell*. 2019;35(6):885–900.e10.
53 Komohara Y, Fujiwara Y, Ohnishi K, Takeya M. Tumor-associated macrophages: potential therapeutic targets for anti-cancer therapy. *Adv Drug Deliv Rev*. 2016;99(Pt B):180–185.
54 Kumar V, Patel S, Tcyganov E, Gabrilovich DI. The nature of myeloid-derived suppressor cells in the tumor microenvironment. *Trends Immunol*. 2016;37(3):208–220.
55 Huang AC, Postow MA, Orlowski RJ, et al. T-cell invigoration to tumour burden ratio associated with anti-PD-1 response. *Nature*. 2017;545(7652):60–65.
56 Miller BC, Sen DR, Al Abosy R, et al. Subsets of exhausted CD8(+) T cells differentially mediate tumor control and respond to checkpoint blockade. *Nat Immunol*. 2019;20(3):326–336.
57 Ribas A, Puzanov I, Dummer R, et al. Pembrolizumab versus investigator-choice chemotherapy for ipilimumab-refractory melanoma (KEYNOTE-002): a randomised, controlled, phase 2 trial. *Lancet Oncol*. 2015;16(8):908–918.
58 Carlino MS, Long GV, Schadendorf D, et al. Outcomes by line of therapy and programmed death ligand 1 expression in patients with advanced melanoma treated with pembrolizumab or ipilimumab in KEYNOTE-006: a randomised clinical trial. *Eur J Cancer*. 2018;101:236–243.